TRACE ELEMENT CARRIER PHASES IN PRIMITIVE CHONDRITE MATRIX: IMPLICATIONS FOR VOLATILE ELEMENT FRACTIONATION IN THE INNER SOLAR SYSTEM. P. A. Bland[1,2], D. Rost[3], E. P. Vicenzi[3], F. J. Stadermann[4], C. Floss[4], M. Fries[5], A. Steele[5], G. K. Benedix[6], M. R. Lee[7], L. E. Watt[1,2] and A. T. Kearsley[2]; [1]IARC, Dept Earth Sci. & Eng., Imperial College London, South Kensington Campus, London SW7 2AZ, UK, p.a.bland@imperial.ac.uk; [2]Dept. Mineralogy, Natural History Museum, Cromwell Road, London SW7 5BD, UK; [3]Dept. Mineral Sci., National Museum of Natural History, Smithsonian Institution, Washington, DC 20560, USA; [4]Laboratory for Space Sci. & Dept Physics, CB 1105, Washington University, Saint Louis, MO 63130, USA; [5]Geophys. Laboratory, Carnegie Institution of Washington, 5251 Broad Branch Road, Washington, D.C. 20015, USA; [6]Dept. Earth & Planetary Sci., Washington University, Saint Louis, MO 63130, USA; [7]Div. Earth Sci., University of Glasgow, Lilybank Gardens, Glasgow G12 8QQ, UK.

Introduction: Volatile element fractionation was one of the earliest and most fundamental processes affecting the inner solar nebula. Solids in the inner Solar System are depleted in volatile elements compared to solar abundances, with moderately volatile elements showing a monotonic depletion in abundance with decreasing condensation temperature. Models to explain volatile depletion in meteorites and the terrestrial planets fall into one of four categories: a) two-component models, with volatile depletion occurring during chondrule formation, and depleted chondrules being mixed with primordial, CI-like matrix [1-3]; b) incomplete condensation during cooling of a hot inner disk, prior to chondrule formation [4-6]; c) evaporative fractionation prior to chondrule formation [7]; or d) inheritance of a volatile-depleted signature from the ISM [8].

Fine-grained matrix is a major (and thermally the most primitive) component in chondrites. Analyses of chondrite matrix [9,10] reveal that although it is enriched in volatile and moderately volatile elements compared to the bulk meteorite, it does not have a primordial CI-like composition, showing instead a consistent depletion compared to solar in all chondrite groups (except CI). Understanding the mineralogy of the volatile and moderately volatile carrier phases in pristine chondrite matrix would inform our choice of model for volatile depletion. For instance, we might expect a mineralogy resembling that predicted by equilibrium condensation during slow cooling of a hot inner disk (b); whereas chondrule formation (a) would be more rapid, with condensates tending to be amorphous and not controlled by equilibrium. However, matrix is rarely pristine. Fine-grained materials experienced variable aqueous, thermal, and impact processing following accretion. Flynn et al. [11] overcame this problem by studying trace element carriers in pristine anhydrous IDPs, with a view to constraining nebula condensation models. We chose to study matrix in Acfer 094, an ungrouped carbonaceous chondrite which largely escaped thermal and aqueous processing [12,13]. Acfer 094 contains presolar silicates [14-16]. If presolar silicates survived asteroidal processing, then condensed materials should also have survived.

Methodology: We used ToF-SIMS, NanoSIMS, Raman, and EDS, to constrain mineralogy, trace element distribution, and oxygen isotopic composition in a 50x50μm area of Acfer 094 matrix. Selected areas will also be analysed by TEM after FIB preparation.

Raman: Analyses were performed at the Carnegie Institution. Confocal Raman imager is a WITec αS-NOM, using a 532nm frequency-doubled YAG laser. Excitation energy is 9mW. Scan size is 130x130 pixels.

ToF-SIMS: Measurements were performed at the Smithsonian Institution using a pulsed 25 kV Ga^+ primary ion beam with a spatial resolution of ~300nm. Complete mass spectra were collected for every pixel in a 256x256 array, including two different mass resolutions for both positive and negative polarities.

NanoSIMS: Oxygen isotopic analyses were performed with the Washington University NanoSIMS in raster imaging mode with parallel detection of $^{16}O^-$, $^{17}O^-$, $^{18}O^-$, and $^{27}Al^-$. Details of analysis are in [16].

Results and Discussion: As noted by Greshake [12], the dominant phases in Acfer 094 matrix are refractory olivine and pyroxene, as well as sulphide, set in an amorphous groundmass (Figure 1). We also observe a variety of new, minor phases. In the following section we discuss associations for specific elements. The expected phases condensing during equilibrium condensation of a solar gas are noted as a guide [17].

Fe, Ni and S: Sulphide is commonly Ni-bearing, as observed by Greshake [12]. FeNi metal is also observed, with variable Ni content across the sample.

Na and K: These elements are co-located, and associated with Al. Based on equilibrium condensation we would expect them to condense in feldspar.

Li: One bright Li hotspot is observed, which does not correlate with Si or Mg (Figure 1). Equilibrium condensation would predict Li in forsterite+enstatite. Instead the host appears to be a Cr- and Ni-bearing phase.

Mn: We would expect Mn in forsterite+enstatite, and in Acfer we find it co-located with Mg and Si, possibly in an enstatite. We also observe a Mn-rich phase with significantly less Si, which appears to be intergrown with a Na&K-rich phase.

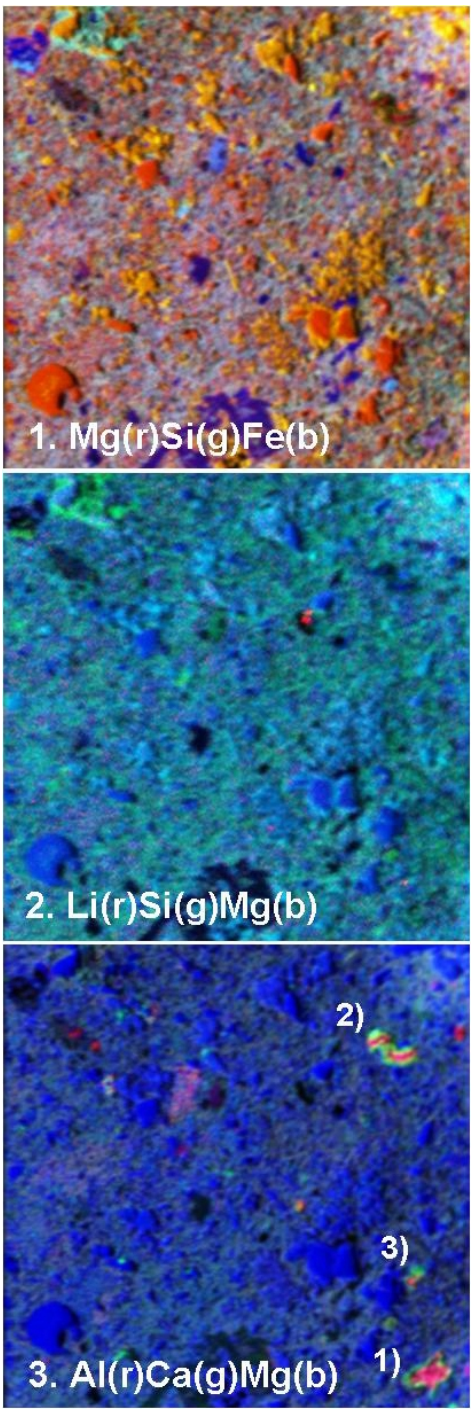

Figure 1. Selected ToF SIMS maps of a 50x50µm area in the matrix of Acfer 094.

Cr: Based on equilibrium condensation we would expect Cr in a Fe alloy. In Acfer, abundant Cr hotspots are observed. The dominant chemistry appears to be Fe and Cr in ~equal proportions: a Cr, Fe alloy.

F and Cl: Equilibrium condensation predicts apatite and sodalite, respectively, as host phases. In Acfer 094 they are associated with a framboidal Fe-oxyhydroxide, possibly ferrihydrite [12] or goethite.

Ca and Al: ToF-SIMS revealed a number of small Ca-Al inclusions. The largest of these (~5µm) are zoned in Ca and Al, and do not appear to be fragments of larger CAIs (CAI1&2 in Figure 1). A 2-3µm inclusion may also be zoned (CAI3 in Figure 1). Smaller objects are observed, with sizes down to the limit of ToF resolution, but it is not possible to determine whether they show any zonation. Oxygen isotopic mapping revealed that CAIs 1&3 are ^{16}O-poor (δ^{17}O: -11±12, δ^{18}O: 6±5; and δ^{17}O: -2±4, δ^{18}O: 6±3, respectively), and CAI 2 ^{16}O-rich (δ^{17}O: -39±2; δ^{18}O: -42±1). Note that these data are normalised to Acfer 094 matrix. We also performed oxygen mapping at the contact between a larger CAI (50µm) and matrix, and note that it is ^{16}O-rich (δ^{17}O: -39±2, δ^{18}O: -42±1), like other large (40-500 µm [18, 19]) CAIs previously described in Acfer 094 [20]. We are currently exploring whether these small CAIs may be a distinct population.

Conclusions: The combination of ToF-SIMS, NanoSIMS, and Raman, provides a powerful new window on the mineralogy and composition of chondrite matrix. Although our data are preliminary, we have significantly expanded the suite of phases observed in Acfer matrix, and identified an unusual set of µCAIs. In terms of volatile depletion, currently the data from Acfer 094 are equivocal: we observe carrier phases for several elements consistent with equilibrium condensation; others (e.g. Li) are not; and an amorphous groundmass [12] suggests disequilibrium condensation. Further work is required to address this question.

References: [1] Anders E. (1964) *Space Sci. Rev., 3,* 583-714. [2] Shu F.H. et al. (1996) *Science, 271,* 1545-1552. [3] Alexander C.M.O'D. et al. (2001) *Science* 293, 64-68. [4] Wasson J.T. & Chou C.-L. (1974) *Meteoritics, 9,* 69-84. [5] Wulf A.V. et al. (1995) *Planet. Space Sci., 43,* 451-468. [6] Cassen P. (1996) *MAPS, 31,* 793-806. [7] Huss G.R. et al. (2003) *GCA, 67,* 4283-4848. [8] Yin Q-Z. (2004) In *Workshop on Chondrites and the Protoplanetary Disk*, pp. 227-288. [9] Bland P.A. et al. (2003) *LPSC XXXIV*, #1750. [10] Bland P.A. et al. (2004) *LPSC XXXV*, #1737. [11] Flynn G.J. et al. (2004) In *Workshop on Chondrites and the Protoplanetary Disk*, pp. 33-34. [12] Greshake A. (1997) *GCA, 61,* 437-452. [13] Greshake A. et al. (2004) In *Workshop on Chondrites and the Protoplanetary Disk*, pp. 51-52. [14] Nguyen A & Zinner E. (2004) *Science, 303,* 1496-1499. [15] Mostefaoui S. & Hoppe P. (2004) *ApJ, 613,* L149-L152. [16] Stadermann F.J. et al. (2005) this conference. [17] Lodders K. (2003) *ApJ, 591,* L1220-L1247. [18] Weber D. (1995) *Meteoritics, 30,* 595-596. [19] Krot A.N. et al. (2004) *GCA, 68,* 2167-2184. [20] Fagan T.J. et al. (2003) *LPSC XXXIV*, #1274.